**AD** 667 156

SPIN RESONANCE IN IRRADIATED PLASTICS

N.R. Lerner

Lockheed Missiles and Space Company
Palo Alto, California

October 1967

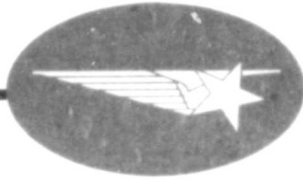*Processed for . . .*

# DEFENSE DOCUMENTATION CENTER
# DEFENSE SUPPLY AGENCY

**CLEARINGHOUSE**

**FOR FEDERAL SCIENTIFIC AND TECHNICAL INFORMATION**

35

AD667156

Technical Report

SPIN RESONANCE IN IRRADIATED PLASTICS

N. R. Lerner

D D C

MAR 1 9 1968

Technical Report

## SPIN RESONANCE IN IRRADIATED PLASTICS

N. R. Lerner

October 18, 1967

## Foreword

This work was performed in conjunction with a broader program aimed at evaluating the response of critical materials to exposure to high dose, nano-second, pulses of electrons. The objectives of this broader program include the study of:

a) chemical events;

b) electrical events;

c) thermomechanical events;

d) the interplay of a), b) and c) in these media as a function of material characteristics and exposure conditions.

The electron spin resonance studies reported here are concerned primarily with the chemical response of plastics to such radiation.

The author gratefully acknowledges the assistance of A. D. King, who irradiated the materials studied, and of E. G. Fritz for many helpful dis-cussions.

1

Abstract

This report contains the results obtained from electron spin reso-
nance studies performed on plastics exposed to high dose, nanosecond,
pulses of electrons. The principal species of free radicals produced in
each plastic studied are identified, and the response of each plastic to
exposure to radiation, at various dose levels as evidenced by the free
radical concentration, is given.

## Table of Contents

iii

Illustrations

## 1. Introduction

In this work electron spin resonance spectroscopy is used as a means of monitoring the chemical response of plastics exposed to high dose, nanosecond pulses of electrons.

The principal radiation-induced changes occurring in plastics have their origin in the rupture of the covalent bonds of the polymer molecules. The rupture of covalent bonds in organic solids frequently leads to the production of free radicals which are trapped in the solids. Free radicals possess an electron with an unpaired spin, and hence give rise to electron spin resonance spectra. The intensity of the electron spin resonance spectrum observed in a sample containing free radicals is directly proportional to the number of free radicals contained in the sample. The structure and shape of the spectrum observed are characteristic of the species of free radical present in the sample.

The eventual aim of the present research is a correlation between the concentration and species of free radicals produced by irradiation with the concomitant changes in the bulk properties of these materials. Such a correlation may ultimately provide a basis for the prediction of the behavior of related engineering materials under arbitrary conditions of radiation exposure.

1

## 2. Experimental Techniques

### 2.1 Exposure of the Samples

#### 2.1.1 Radiation Source

The Febetron 705[*] (Field Emission electron generator) was the source of high-dose, nanosecond pulses of electrons.

The Febetron is a high voltage radiation source. At full voltage the extracted electron beam has an average current density of 1000 $amp/cm^2$. The beam energy density per 20 nanosecond pulse exceeds 60 $joules/cm^2$ and the maximum β-ray surface dose is 9 megarads per pulse. At full voltage the maximum energy of the electrons is 2 Mev.

The decrease in energy density of the beam from the Febetron follows an inverse squared distance law at distances greater than 10 cm. At distances less than 10 cm. it exhibits a nonlinear behavior.

#### 2.1.2 Handling of the Samples

The samples to be irradiated were cut in the form of small cylinders (0.10 inch in diameter and 0.25 inch in length).

The samples were exposed to the beam from the Febetron in a phenolic holder. The holder was constructed so that a thin sheet of plastic could be placed directly in front of the sample for dosimetry. The dose the samples received was controlled by varying the distance of the samples from the window of the Febetron.

After irradiation the samples were placed in quartz tubes which were sealed off and placed immediately in liquid nitrogen.

---

[*] Manufactured by the Field Emission Corp., McMinnville, Oregon.

2

2.1.3  Dosimetry

Strips of Cinemoid #48 Bright Rose Filter (Cinemoid Filter) were

used as dosimeters.  The optical density at 520 mμ of the Cinemoid filters

was measured with the Beckman D.U. spectrophotometer both before and after

irradiation.  The change in optical density was computed and the dose that

this change corresponded to was found from a calibration chart.  The cali-

bration chart was prepared by comparing the change in optical density of the

Cinemoid filters with dose as measured by an aluminum calorimeter.

3

2.2 The Spin Resonance Measurement Procedure

The procedure used to determine the amount and species of free radicals present in the plastics prior to, and after irradiation, was electron spin resonance spectroscopy.

In these experiments, a plot of the first derivative of the paramagnetic resonance absorption versus magnetic field was obtained, $\left(\dfrac{dA}{dH}\right)$ vs H.

The free radical species present in the samples were identified by the line shape and by hyperfine structure if it was present.

The amount of free radicals present in each sample was measured in the following manner:

1) The derivative of the absorption curve of the sample vs field was obtained.

2) With the sample remaining in the cavity, the peak-to-peak height of the resonance (signal intensity) due to a single crystal of ruby placed in a fixed position in the cavity was obtained.

3) The resonance curve of the sample was integrated to obtain the absorption curve. The area under the absorption curve was calculated and the ratio,

   K(sample) = area under the absorption curve/signal intensity ruby computed.

4) To find what spin concentration this ratio corresponds to, a sample of known concentration of DPPH was placed in the cavity. Its resonance curve and the signal intensity of the ruby were measured. The ratio

$$\frac{\text{Area under the absorption curve (DPPH)}}{\text{signal intensity (Ruby)}} = (K_{DPPH})$$

was calculated.

4

5) The spin concentration was then calculated.

$$\text{spin concentration} = \frac{K\,(\text{sample})}{K_{DPPH}} \times \text{concentration}\,(DPPH)$$

For samples of the same species of free radical the ratio

$$\frac{\text{Area under the absorption curve (sample)}}{\text{signal intensity (sample)}} = \text{a constant}$$

We have calculated this constant for a large number of samples containing the same species of free radicals, and then we have used the average value of this constant to obtain the value of the area under the absorption curve for the other samples containing this species. This decreases our error in integration, because we can use samples to obtain the value for this constant whose signal-to-noise ratio is high, thus having a smaller error in integration than we do in integrating noisy derivative curves (see section on error).

All samples were measured at liq $N_2$ temperature unless stated otherwise.

2.3  Sources of Error

The main sources of error are:

a)  Sample position:

The signal intensity produced by a sample depends on the amplitudes of the r.f. magnetic field at the sample, and the modulation field at the sample. Both of these quantities fall off rapidly as the sample is displaced from the center of the cavity, i.e., the portion of the sample which is furthest from the center of the cavity contributes less

5

to the signal intensity than those which are nearer. Hence, samples of the same size and shape, positioned at the same point in the cavity, must be compared. Since the ratio of the signal height of the same sample to that of the Ruby standard should remain constant, the accuracy with which this ratio can be reproduced as the sample is removed from the cavity and then returned to the same position is a measure of the error due to sample positioning. This error was determined to be $\pm 5\%$.

b) Integration Error

   1. Zero drift and noise. The accuracy with which the absorption curve can be calculated depends on the accuracy with which the derivative of the absorption curve can be measured. This accuracy varies from sample to sample, because samples with a low concentration of spins must be observed at higher gains, thus the noise level is increased.

   2. Accuracy in measurement of the sweep rate. In our experimental setup, the primary data obtained is a plot of derivative of absorption with respect to field versus time. If the sweep rate $\left( \frac{dH}{dt} \right)$ is a constant during the time one sweeps through a resonance line, the plot of $\frac{dA}{dH}$ versus time may be converted into a plot of derivative of absorption versus magnetic field via measuring the

6

sweep rate. The experimentally obtained resonance curve may then be integrated graphically, that is, a plot is made of

$$A(H_n) = \sum_{i=1}^{n} \left( \frac{dA}{dH} \right)_{\frac{i}{2}} \Delta H_i \tag{1}$$

where:

$A(H_n)$ is the value of the absorption when the magnetic field has the value $H_n$.

$\left( \frac{dA}{dH} \right)_{\frac{i}{2}}$ is the average value of the derivative of the absorption in the interval between $H_i$ and $H_{i-1}$.

$\Delta H_i$ is the difference $H_i - H_{i-1}$.

If the sweep rate is constant

$$\Delta H_i = \frac{dH}{dt} \Delta t_i \text{ and } H_n = \left( \sum_{i=1}^{n} \frac{dH}{dt} \Delta t_i \right) + H_0. \tag{2}$$

We see from (1) that the height of the absorption curve and the width of the absorption curve are directly proportional to the sweep rate. Thus the area under the absorption curve depends upon the square of the sweep rate. The error in calculating the area under the absorption curve due to an inaccuracy in the measurement of the sweep rate is

$\left( \frac{dH}{dt} \right) \Delta \frac{dH}{dt}$ , where $\Delta \frac{dH}{dt}$ is the error in measuring the sweep rate.

3. Computing the integration error. Since for one substance the ratio

7

$$\frac{\text{Area under the absorption curve}}{\text{signal intensity}} = \text{a constant,}$$

We have computed this ratio for a large number of samples of the same substance and found the average value. We have taken our error in integration for each substance to be the average deviation of the mean.

3. Results

3.1 Teflon

The samples of Teflon were studied prior to irradiation and no signals were observed in the unirradiated samples. The sensitivity of the apparatus was such that free radicals of a concentration of $10^{14}$ spins/cc could have been observed.

After irradiation, an E.S.R. spectrum was observed in the samples of Teflon at liquid nitrogen temperature. Ovenall[1] has observed an E.S.R. spectrum in stretched samples of Teflon irradiated in air. Our spectrum at liquid nitrogen temperature is similar to the one he observed a. liquid nitrogen temperature when the magnetic field is oriented perpendicular to the elongation direction. He also observed an E.S.R. spectrum at room temperature which differed from that observed at liquid nitrogen temperature. We obtain similar results at room temperature. Ovenall attributes the spectra he observes to the radical $-\text{C}^{F_2} - \underset{O-O}{\overset{F}{\text{C}}} - \text{C}^{F_2} - $ . A typical E.S.R. spectrum as observed at liquid nitrogen temperature is illustrated in Fig. 1. The asymmetry of the line shape is due to an anisotropy in the g values ($g_{\perp}$ = 2.002 and $g_{\parallel}$ = 2.04, the parallel direction being along the oxygen bond).

We have studied the variation of the E.S.R. spectrum of Teflon with temperature from room temperature to liquid nitrogen temperature.

---

[1] Ovenall, J. Chem. Phys. 38, 2448 (1963).

Typical spectra obtained are shown in Figures 2-4. We observed that the line shape varies continuously from liquid nitrogen temperature to room temperature. We tentatively attribute the variation to the vibration of the peroxide group about the polymer chain.

The results of the measurement of spin densities for the Teflon samples are tabulated in Table I. The error in integration for the Teflon samples was $\pm$ 10%. The error in calibrating the ruby standard with DPPH was $\pm$ 20% and the positioning error is assumed to be $\pm$ 5%. The total error is assumed to be $\pm$ 35%.

## Table I

### SUMMARY OF TEFLON RESULTS

| Sample | Distance (cm) | Dose (Mrad) | Spin/cc ($x\ 10^{-18}$) |
|--------|---------------|-------------|--------------------------|
| 671 | 1.5 | 4.9 | 1.46 |
| 672 | 1.5 | 5.0 | 1.64 |
| 673 | 1.5 | 5.5 | 1.70 |
| 675 | 2.8 | 2.7 | .99 |
| 676 | 2.8 | 3.4 | .80 |
| 678 | 4.5 | 2.4 | .44 |
| 679 | 4.5 | 2.4 | .58 |
| 680 | 8.5 | 1.5 | .40 |
| 681 | 8.5 | 1.8 | .38 |
| 682 | 8.5 | 1.9 | .42 |
| 683 | 50.0 | .24 | .14 |
| 684 | 50.0 | .30 | .12 |
| 685 | 50.0 | .26 | .18 |

## 3.2  High Density Polyethylene

The samples of high density polyethylene were studied prior to irradiation and no free radicals were observed in them (sensitivity $10^{14}$ spins/cc).

Upon irradiation, free radicals were observed in all the samples studied. At high dosages (Fig. 5), the E.S.R. spectrum consisted of a 7-line spectrum superimposed on a broad central line. The principal species produced were the allyl radical, $-\overset{H_2}{C} - \overset{\cdot}{CH} - \overset{H}{C} = \overset{H}{C} - \overset{H_2}{C} - $ which is characterized by a 7-line hyperfine pattern (hyperfine splitting 18 gauss)[1, 2, 3] and the polyenyl radical $-\overset{H_2}{C} - \overset{\cdot}{CH} - ( - CH = CH - )_n - CH_2 - $ which goes to a single line whose width is inversely proportional to n.[3] Both the polyenyl radical and the allyl radical have been observed to be produced in preference to the alkyl radical at high dose ($10^7 - 10^8$ rad).[3]

At intermediate doses, in addition to the polyenyl radical and the allyl radical, we observed the alkyl radical, $- \overset{H_2}{C} - \overset{C}{\underset{\cdot}{C}} - \overset{H_2}{C} - $ , (see Figure 6 and 7). This species is characterized by a 6-line hyperfine pattern (hyperfine splitting 30 gauss)[1]. Its presence can be detected by the fact that the outermost peaks of its hyperfine pattern lie outside of the pattern produced by the allyl and polyenyl radicals.

At low dose, the E.S.R. spectrum seemed to be due to the alkyl radical alone (see Fig. 7). This is in accord with the results of Ohnishi et. al., who observe that the alkyl radical is produced preferentially at low doses ($10^6$ rad and less)[3].

An attempt was made to calculate the concentration of the alkyl radical in the samples by assuming the ratio

$$\frac{\text{Area under the absorption curve(alkyl)}}{\text{height outermost peak}} = \text{a constant}$$

11

The results of the E.S.R. studies on high density polyethylene are tabulated in Table II. Because of the variation in the relative concentrations of the species of free radical in the sample, we estimate that the integration error here is at least $\pm$ 20% leading to a total error of at least 45%.

## Table II

### SUMMARY OF HIGH DENSITY POLYETHYLENE RESULTS

| Sample | Distance (cm) | Dose (M rad) | Spins/cc $(x\ 10^{-18})$ | % Alkyl |
|---|---|---|---|---|
| 687 | 1.5 | | .33 | |
| 688 | 1.5 | 4.5 | .36 | |
| 689 | 2.8 | 4.8 | .42 | |
| 690 | 2.8 | 3.2 | .44 | |
| 691 | 2.8 | 5.4 | .42 | 22 |
| 692 | 4.5 | 2.1 | .42 | 25 |
| 694 | 4.5 | 2.3 | .45 | 31 |
| 695 | 8.5 | 1.9 | .29 | 27 |
| 696 | 8.5 | 1.9 | .37 | 34 |
| 697 | 8.5 | 2.4 | .51 | 42 |
| 698 | 50.0 | .48 | .069 | 100 |
| 699 | 50.0 | .30 | .075 | 90 |
| 700 | 50.0 | .82 | .081 | 100 |

1.  S. Ohnishi, S. Sugimoto, and I. Nitta, J. Chem. Phys. 39, p. 2647 (1963).
2.  S. Ohrishi, Y. Ikeda, M. Kashiwayi and I. Nitta, Polymer 2, 119 (1961).
3.  S. Sugimoto, and I. Nitta, J. Polymer Sci. 47, 503 (1960).

## 3.3 Low Density Polyethylene

The low density polyethylene samples were studied prior to irradiation and no free radicals were detected (sensitivity $10^{14}$ spins/cc).

After irradiation, the species found to be present were the polyenyl radical $- H_2C - \underset{H}{\overset{H}{C}} - ( - CH = CH - )_n - CH_2 -$ and the allyl radical $- H_2C - \overset{\cdot}{C} - CH = CH - CH_2 -$ (compare Figures 5 and 8). The central line due to the polyenyl radical, has grown so as to obscure part of the hyperfine pattern of the allyl radical. From the absence of any peaks at 3330 gauss and at 3180 gauss, we conclude that no alkyl type radicals were present in any of the samples.

At low doses, the central peak attributed to the polyenyl radical is even more pronounced and only the outermost peaks of the hyperfine pattern due to the allyl radical are discernible. This is in opposition to the results of Ohnishi et. al. (see ref. 3 in section on high density polyethylene), who find that the allyl radical is produced in preference to the polyenyl radical at low doses, and at high doses the production of the polyenyl radical predominates.

The concentration of free radicals observed in low density polyethylene are tabulated in Table III. The integration error is $\pm$ 10% leading to a total error of $\pm$ 35%.

13

Table III

SUMMARY OF LOW DENSITY POLYETHYLENE RESULTS

| Sample | Distance (cm) | Dose (M rad) | Spins/cc $(x\ 10^{-18})$ |
|--------|---------------|--------------|--------------------------|
| 701 | 1.83 | 2.7 | .133 |
| 702 | 1.83 | 3.0 | .113 |
| 703 | 1.83 | 3.1 | .090 |
| 704 | 3.35 | 2.2 | .100 |
| 705 | 3.35 | 2.2 | .099 |
| 706 | 3.35 | 2.2 | .088 |
| 707 | 5.7 | 1.6 | .112 |
| 708 | 5.7 | 1.5 | .104 |
| 709 | 5.7 | 1.5 | .098 |
| 710 | 14.0 | .59 | .095 |
| 711 | 14.0 | .62 | .110 |
| 713 | 47.5 | .10 | .066 |
| 714 | 47.5 | .18 | .054 |
| 715 | 47.5 | .11 | .070 |

3.4  Polyphenylene

The samples of polyphenylene were studied prior to irradiation and free radicals were observed in them (see Figure 10). The concentration of free radicals in the samples appeared to be uniform to within experimental error ($\pm$ 30%) and was 4.5 x 10$^{15}$ spins/cc.

Upon irradiation the signal grew in intensity but no new species appeared to be produced (compare Figs. 10 and 11). With the larger signal-to-noise ratio, due to the greater spin concentration, it was possible to observe the spectrum using a smaller modulation field. When this was done, an unresolved

hyperfine pattern consisting of four discernible peaks, became apparent (see Fig. 12). Decreasing the amplitude of the modulation further did not improve the revolution of the hyperfine pattern. The hyperfine splitting appeared to be approximately 6 gauss or less. The identification of the free radical or free radicals observed in polyphenylene is made difficult by the lack of previous ESR investigations of the polyphenyls.

Buben et. al.[1] have observed an ESR spectrum from irradiated diphenyl. The free radicals produced give rise to a triplet spectrum. These authors do not give the magnitude of the hyperfine splitting nor do they identify the free radical observed.

Upon irradiating solid benzene Ohnishi et. al.[2] observe an ESR spectrum which is characterized by:

a) a triplet (hyperfine splitting 47.5g),

b) each line of the triplet is further split into a quartet (hyperfine splitting 11.5 gauss).

They attribute the observed spectrum to the hexadienyl radical
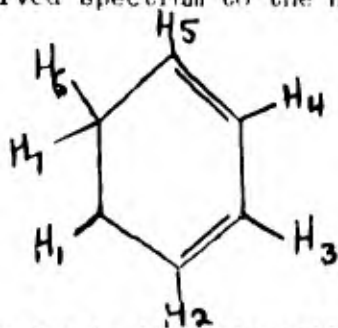


The triplet splitting is due to the interaction of the unpaired electron with the $H_6$ and $H_7$ protons and the quartet splitting is due to the interaction of the unpaired electron with the $H_1$ $H_5$ and $H_3$ protons. They also believe that the phenyl radical is produced because of the strong intensity of the central line of the observed spectrum.

15

Bennet and Thomas[3] have prepared the phenyl radical by chemical reaction. These authors observe that the phenyl radical gives a three component spectrum (hyperfine splitting 19 gauss).

Dixon[4] predicts the following coupling constants for the phenyl radical (considering negative overlap integrals):

$$a_{ortho} = 23.3 \text{ gauss}$$

$$a_{meta} = 4.2 \text{ gauss}$$

$$a_{para} = 17.9 \text{ gauss}.$$

If negative overlap integrals are neglected, the predicted hyperfine coupling constants are:

$$a_{ortho} = 19.2 \text{ gauss}$$

$$a_{meta} = 3.1 \text{ gauss}$$

$$a_{para} = 0.1 \text{ gauss}.$$

The spectrum we observed is characterized by the absence of a triplet hyperfine structure. In view of the results of Ohnishi and the narrowness of the line we observed it can be assumed that the free radical produced is not of the hexadienyl type. The magnitude of the hyperfine splitting observed ($\sim$ 6 gauss) indicates the absence of protons ortho to the missing proton if one assumes a phenyl type radical is the one observed.

Before a definite assignment of the free radicals present can be made more work is necessary on polyphenyls is necessary.

The spin concentrations for polyphenylene are given in Table IV. The integration error is 10% leading to a total error of 35%.

16

## Table IV

### SUMMARY OF POLYPHENYLENE RESULTS

| Sample | Distance (cm) | Dose (M rad) | Spins/cc $(x\ 10^{-18})$ |
|---|---|---|---|
| 716 | 1.83 | 3.2 | .204 |
| 717 | 1.83 | 3.3 | .324 |
| 718 | 1.83 | 3.2 | .304 |
| 719 | 3.35 | 2.2 | .183 |
| 720 | 3.35 | 1.9 | .353 |
| 721 | 3.35 | 2.3 | .376 |
| 722 | 5.7 | 1.5 | .185 |
| 723 | 5.7 | 1.5 | .376 |
| 724 | 5.7 | 1.5 | .350 |
| 725 | 14.0 | .52 | .151 |
| 726 | 14.0 | .58 | .360 |
| 727 | 14.0 | .66 | .370 |
| 728 | 47.5 | .24 | .115 |
| 729 | 47.5 | .19 | .256 |
| 730 | 47.5 | .14 | .169 |

17

# REFERENCES

1.  N. Y. Buben, I. I. Chkheidze, A. T. Koritzky, Y. N. Molin, V. N. Shamshev, V. V. Voenodsky, The Fifth International Symposium on Free Radicals, Uppsala 1961, paper No. 46.

2.  Ohnishi, Tanei, and Nitta, J. Chem. Phys. $\underline{37}$, p. 2404 (1962).

3.  Bennett, and Thomas, Proc. Roy. Soc. (London) $\underline{280A}$, p. 123 (1964).

4.  W. T. Dixon, Molecular Physics, $\underline{2}$, (3), p. 208 (1965).

4. Conclusions

We observed in the case of hydrocarbon polymers that the free radical concentration increased very rapidly with dose up to doses of appoximately 1. Mrad. At doses above 1. Mrad the free radical concentration produced by irradiation remained constant (see Figures 14-16).

Hydrocarbon polymers irradiated under steady state conditions have been observed to exhibit a linear relationship between spin concentration and dose at these dose levels.[1-4] We hypothesize that the saturation of the spin concentration observed in hydrocarbons irradiated at high dose rates is due to the concomitant heating of the samples. Such heating would tend to promote the reaction of the free radicals. The results on Teflon (poly-tetrafluoroethylene) tend to support our hypothesis. Teflon was found to exhibit a linear relationship between spin concentration produced by irraida-tion and dose received. The higher atomic weight of the fluorine atoms would tend to inhibit the motion of the free radicals in this solid and hence their reaction would be less likely to occur.

The predominant result of free radical reaction in polyethylene, for example, is crosslinking of the polymer chains.[5] Crosslinking in polymers leads to greater rigidity and a higher softening point. In view of our re-sults, it would be expected that polymers irradiated at high dose rate would exhibit a greater degree of crosslinking than those irradiated to the same dose under steady state conditions, and that this would be strongly reflected in their mechanical properties.

# REFERENCES

1. Charlesby, A., Libby, D., and Ormerod, M. G., Proc. Roy. Soc. A262, p. 207 (1961).

2. Lawton, E. J., Balwit, J. S., and Powell, R. S., J. Chem. Phys., 33, 395 (1960).

3. Koritskii, A. T., Molin, Y. N., Shamishev, V. N., Buben, N. Y., and Voevodskii, V. V., 1959, Vysokomol. Swed., 1, 1182.

4. Atwater, H. A., J. Applied Physics, 36, p. 2220 (1965).

5. Charlesby, A., and Ormervod, M. G., The Fifth International Symposium on Free Radicals, July 6-7, 1961, Gordon and Breach Science Publishers, Inc., New York, 1961, pp. 11-1 — 11-23.

5. Plans for Future Work

   a) A correlation will be made between our observations and the changes
      in mechanical properties produced in plastics upon irradiation.[1]

   b) All the irradiations reported in this work have been carried out
      in air. To assess the effect of atmospheric gases on the radia-
      tion damage mechanism in polymers, studies are planned on materials
      that have been irradiated in vacuum.

   c) Studies are also planned on samples irradiated at liquid nitrogen
      temperature, in order to eliminate effects due to heating of the
      samples.

   d) Studies will be made on the mechanism of decay of the free radicals
      produced in plastics.

   e) We plan to exploit the linear relationship found between the spin
      concentration produced in Teflon and dose received for dosimetric
      purposes.

---

[1] Studies are currently being conducted by our group on the change in
mechanical properties of plastics that have been subjected to irradiation
in the Febetron.
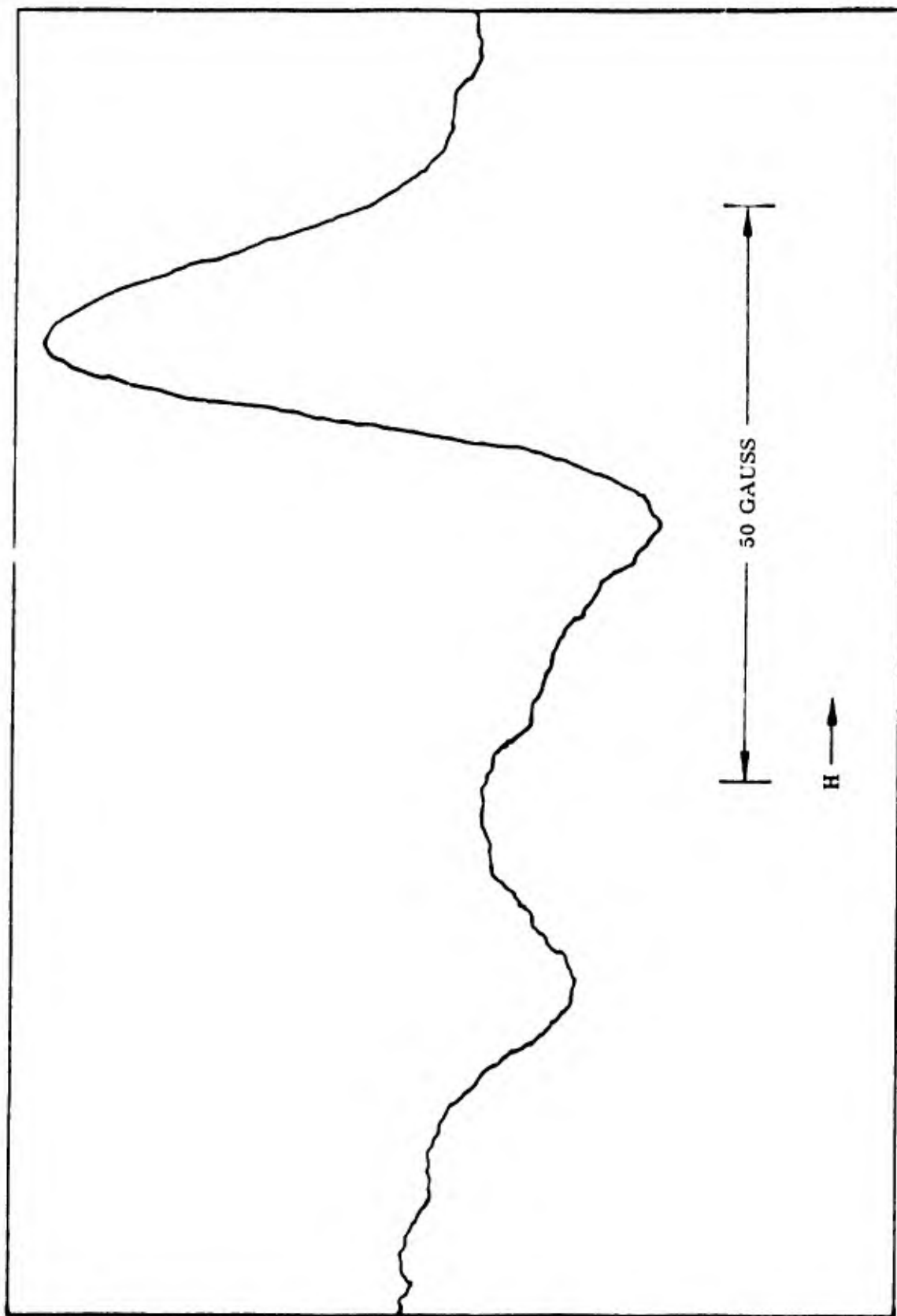
Fig. 1 E.S.R. spectrum of irradiated Teflon at -196°C.
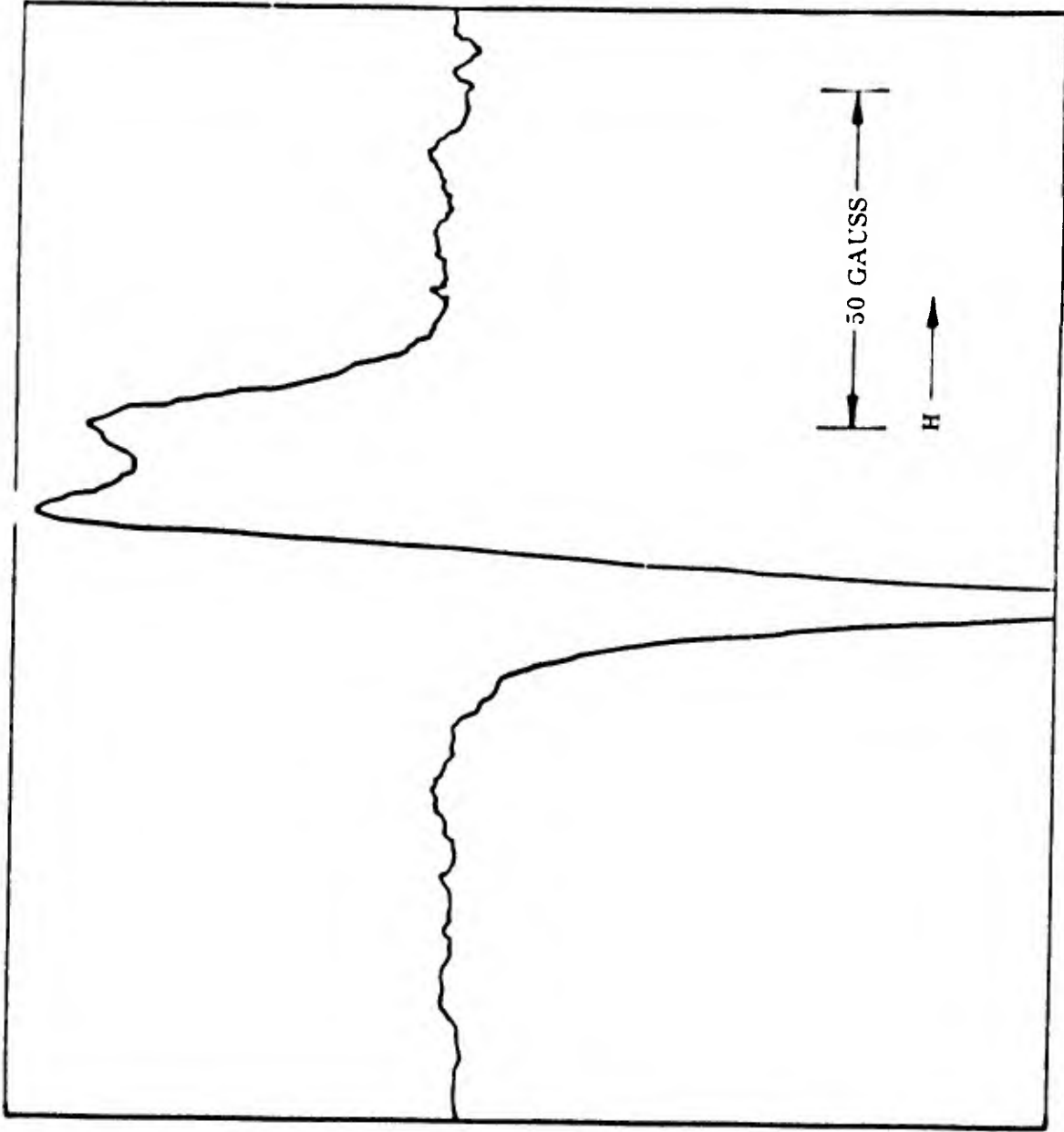
Fig. 2  E.S.R. Spectrum of irradiated Teflon at 22°C.

50 GAUSS

H
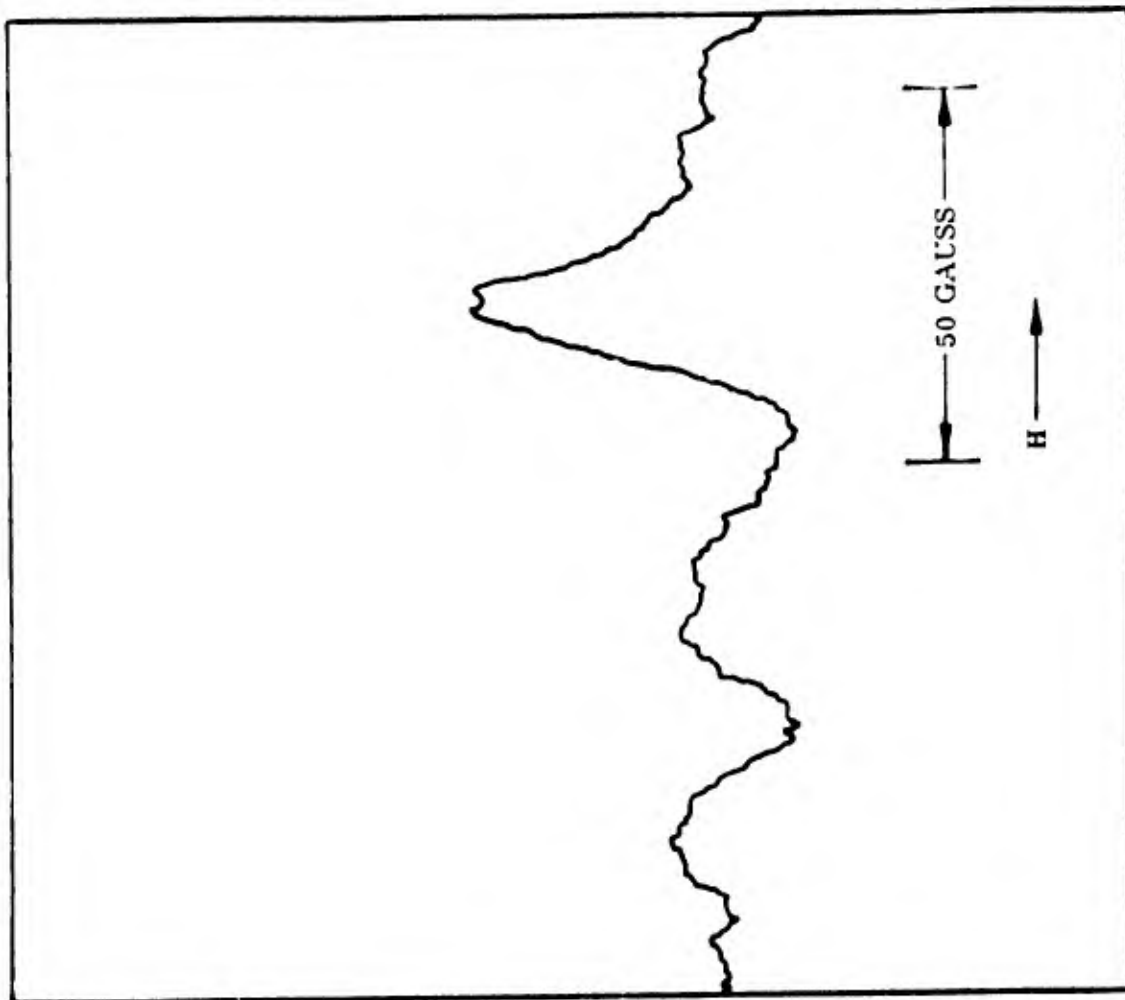
Fig. 3  E.S.R. spectrum of irradiated Teflon at -175°C.

50 GAUSS

H
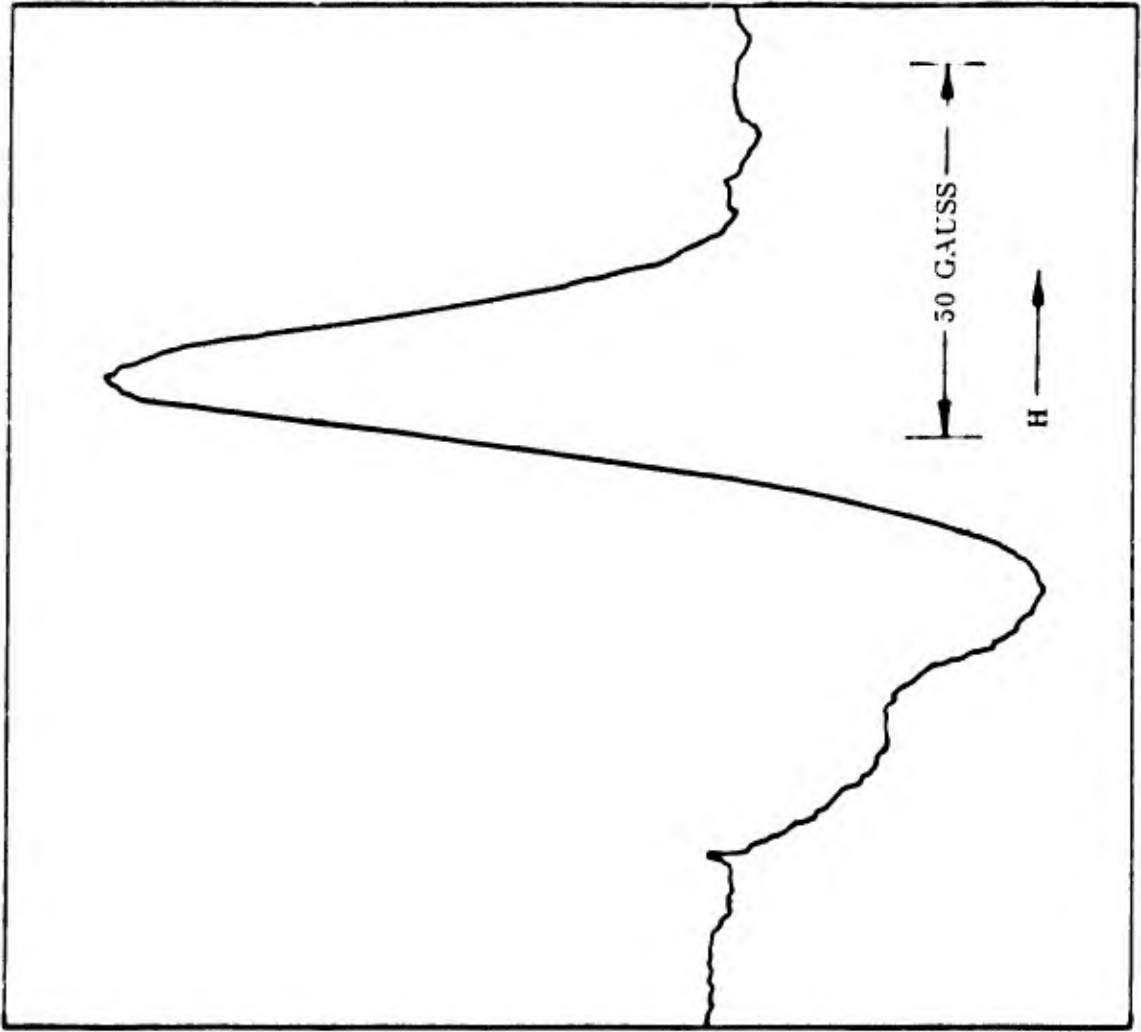
Fig. 4  E.S.R. spectrum of irradiated Teflon at -96°C.

50 GAUSS

H
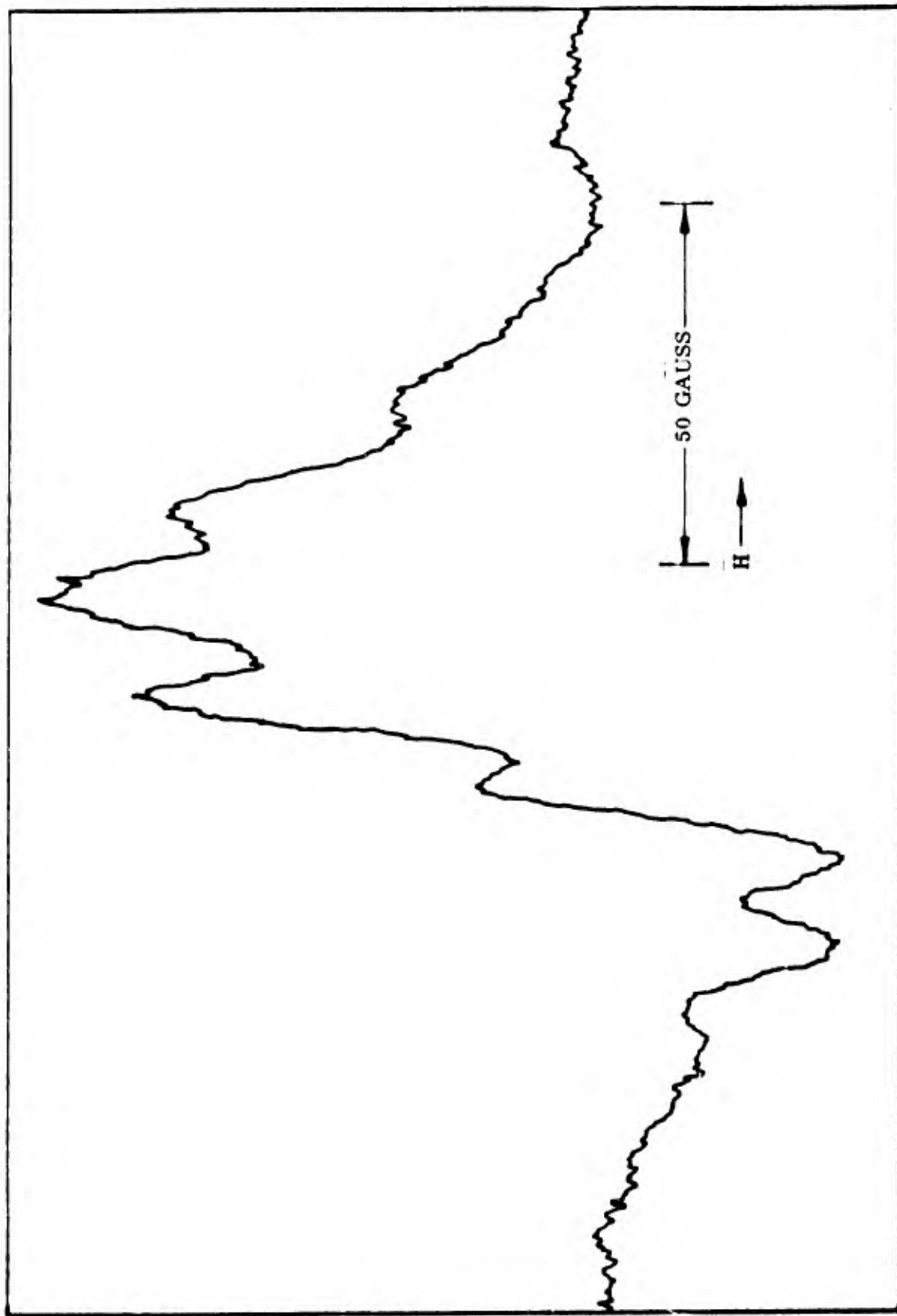
Fig. 5  E.S.R. spectrum at -196°C of high density polyethylene irradiated

to a dose of 3.2 Mrad.
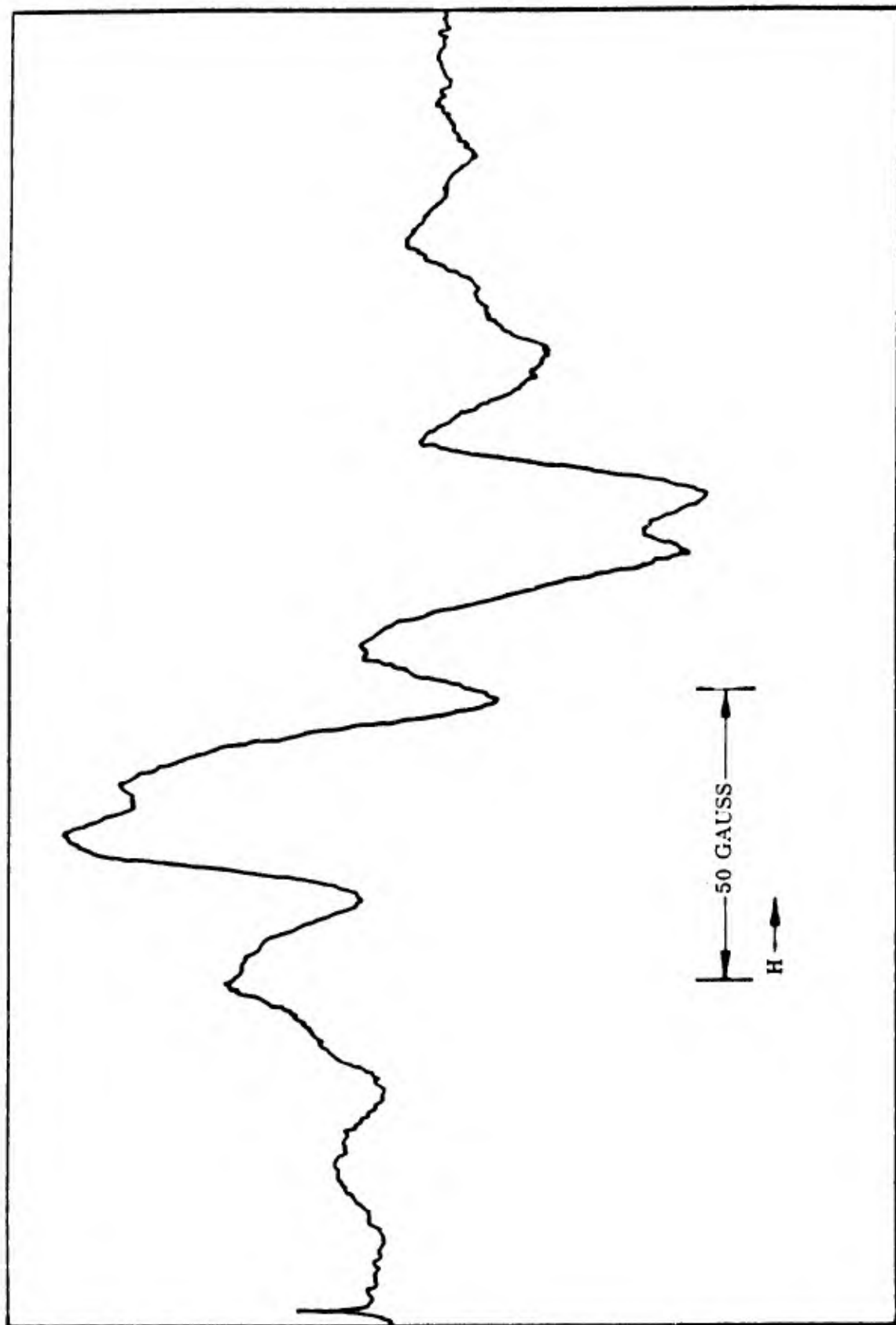
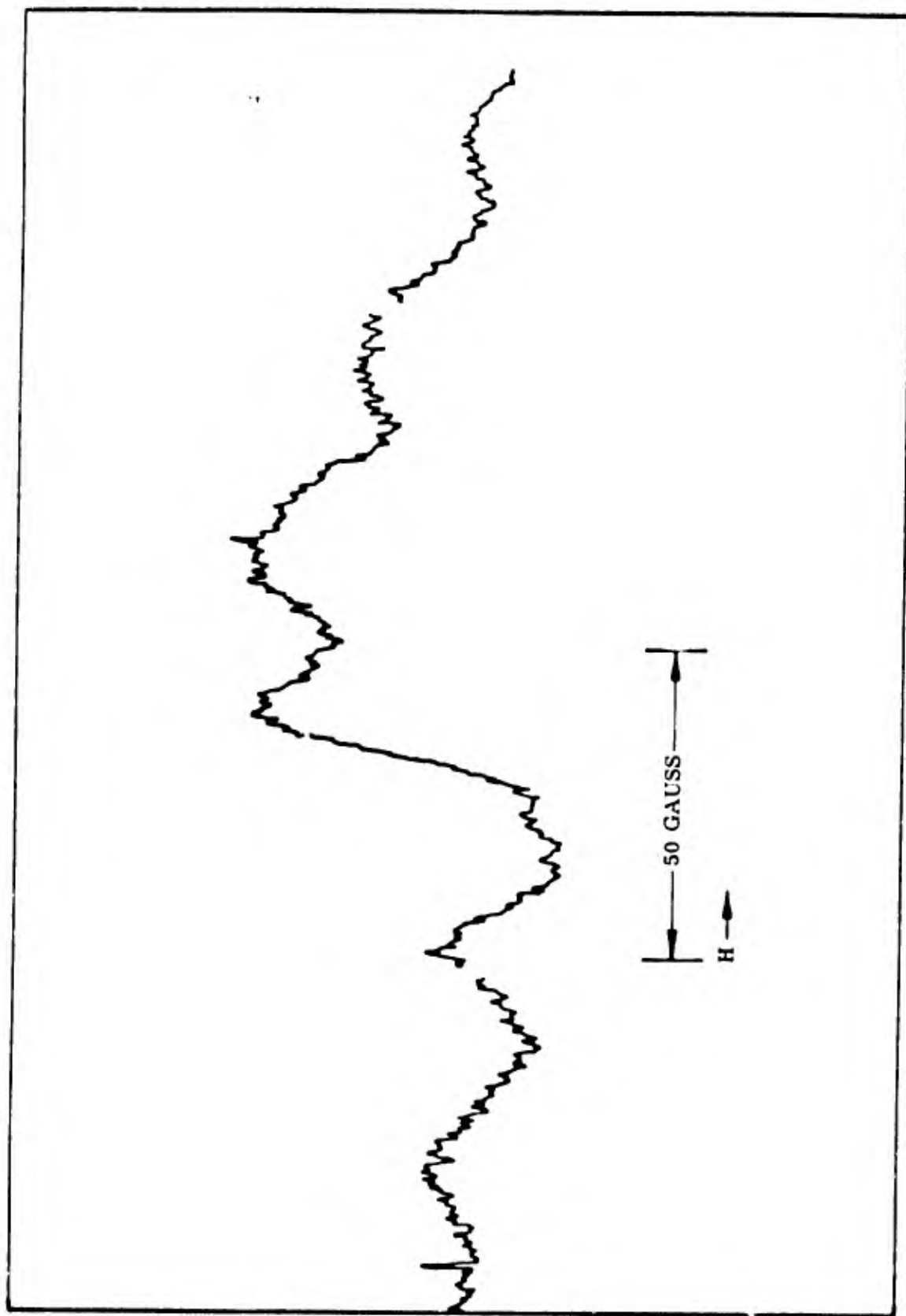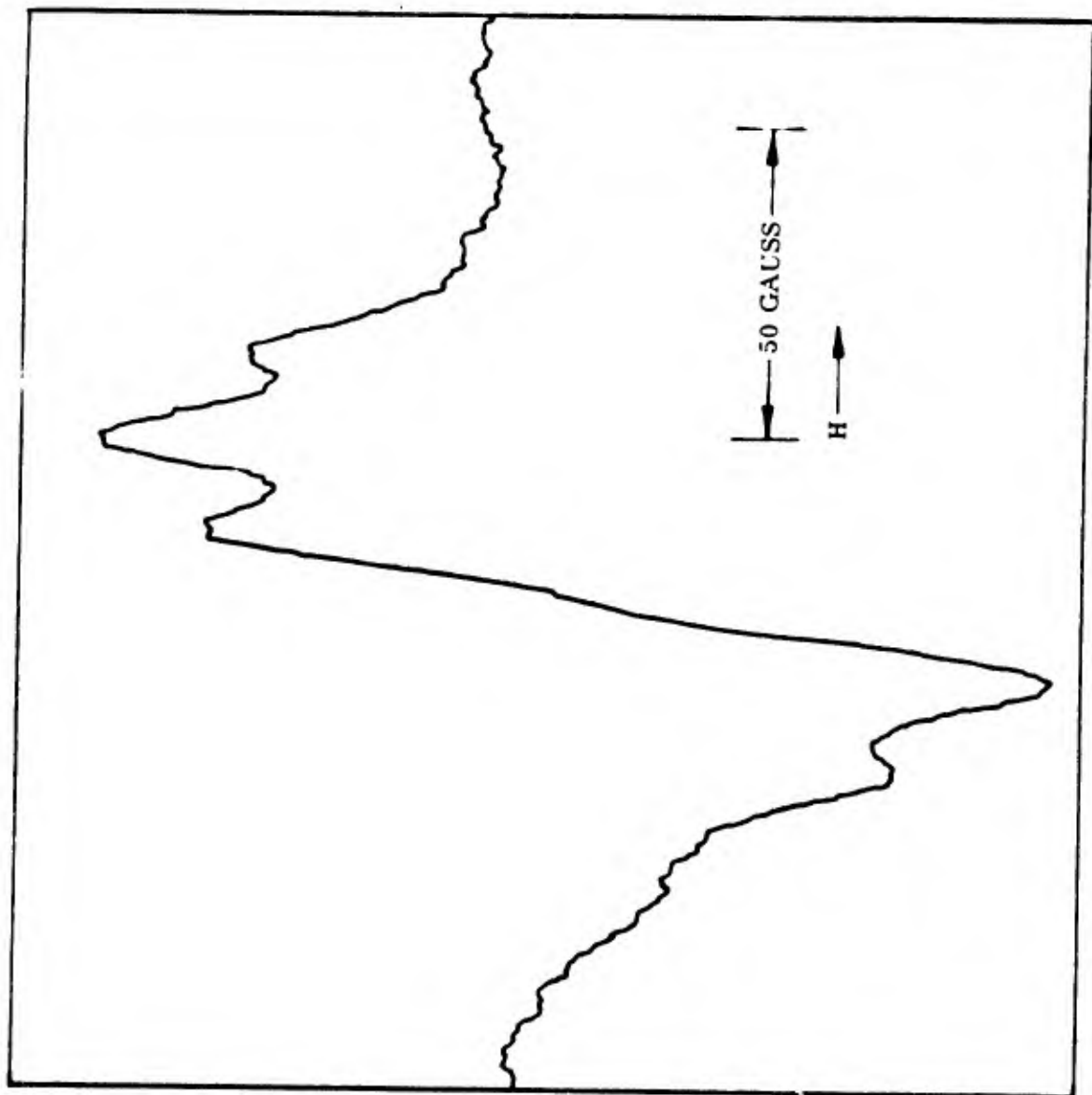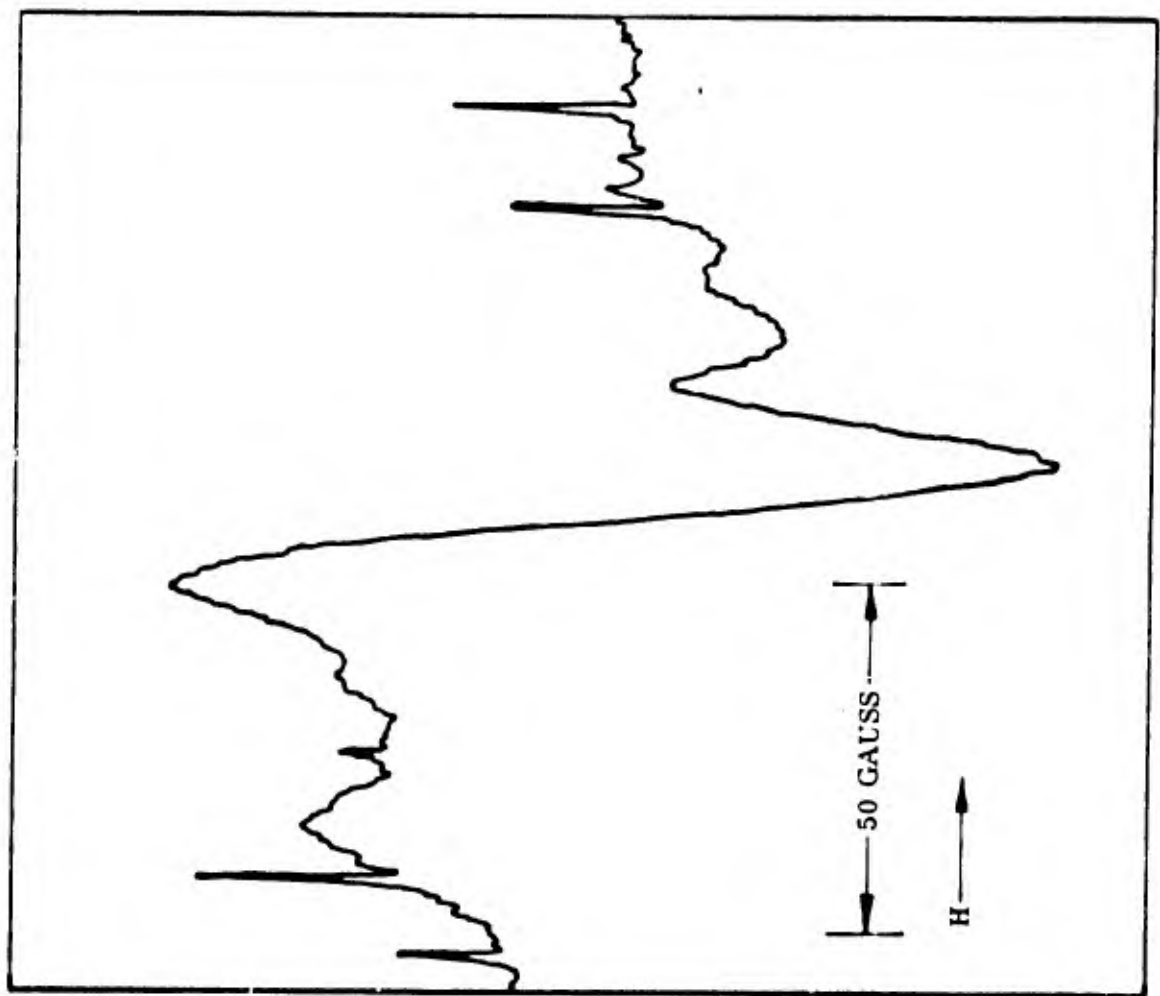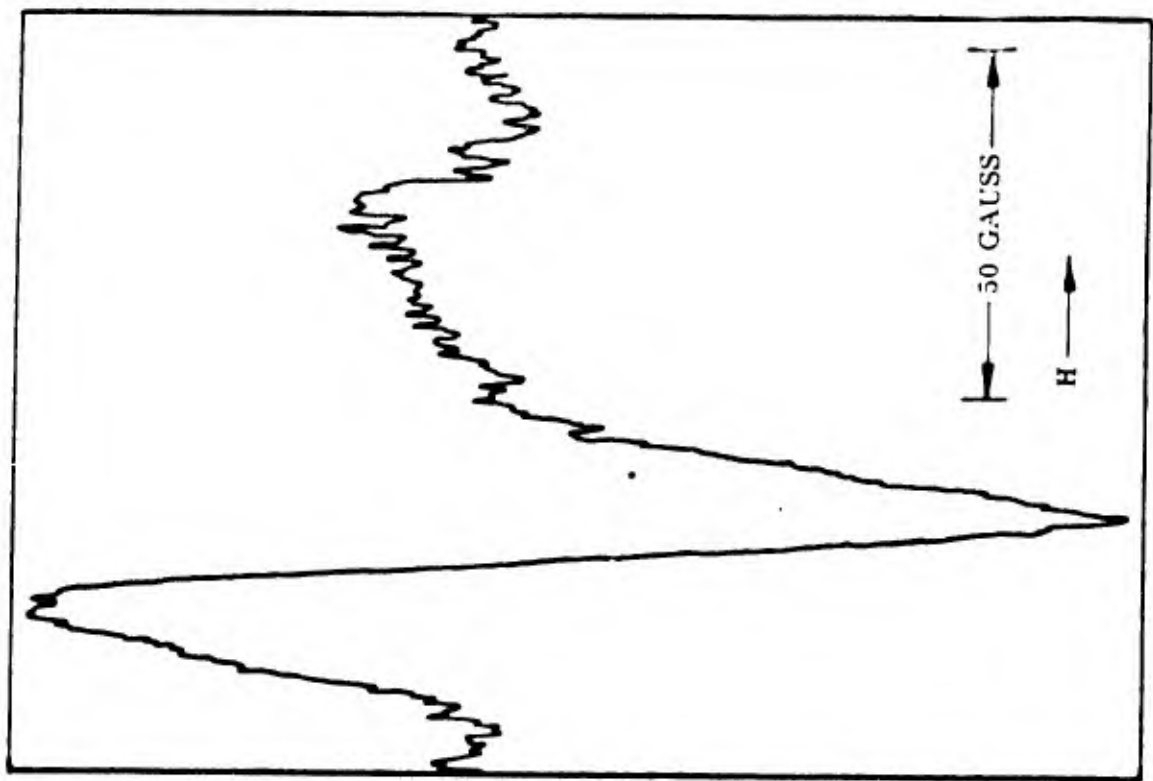Fig. 6  E.S.R. spectrum at -196°C of high density polyethylene irradiated to a dose of 2.4 Mrad.

Fig. 7  E.S.R. spectrum at -196°C of high density polyethylene irradiated to a dose of .30 Mrad.

50 GAUSS

H

Fig. 3 E.S.R. spectrum at -196°C of low density polyethylene irradiated at a dose of 2.3 Mrad.

Fig. 9 E.S.R. spectrum at -196°C of low density polyethylene irradiated at a dose of .10 Mrad.

Fig. 10 E.S.R. spectrum of polyphenylene prior to irradiation.
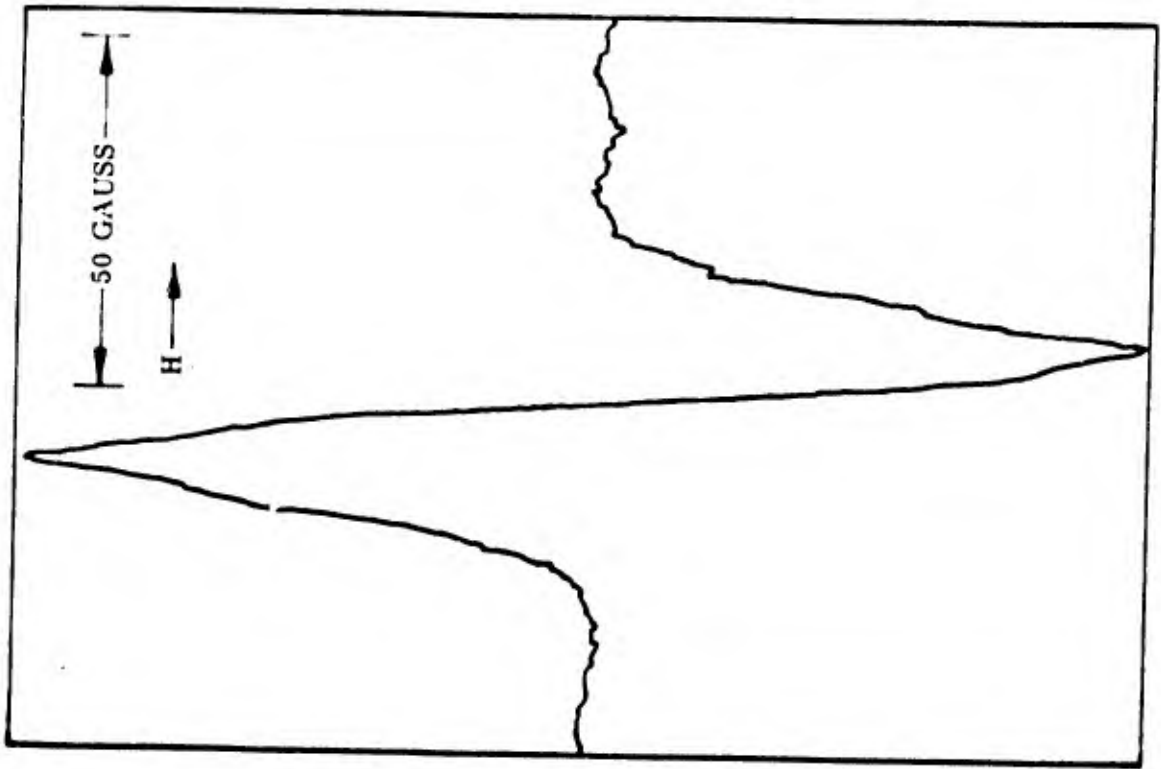
Fig. 11  E.S.R. spectrum of irradiated polyphenylene.
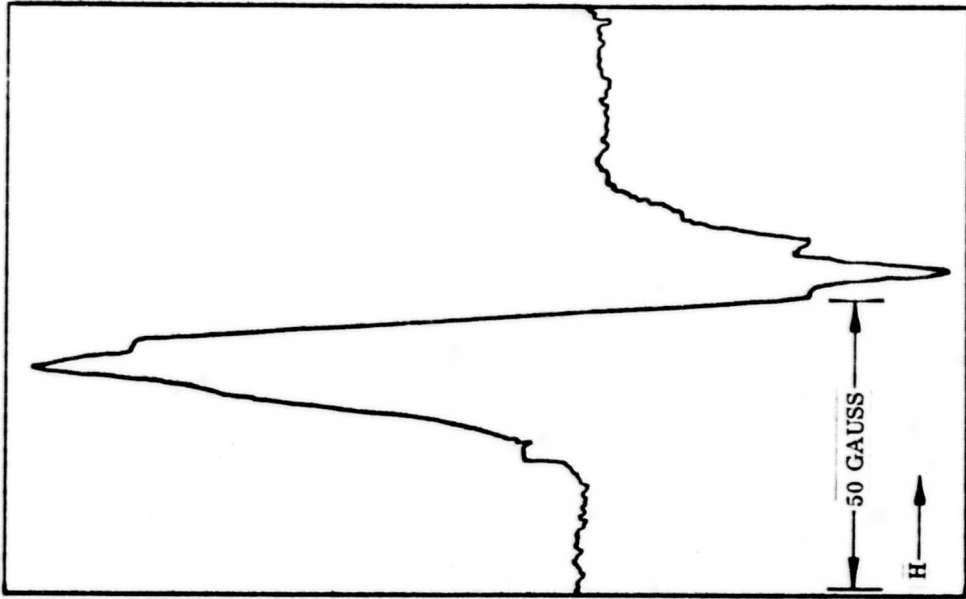
Fig. 12  E.S.R. spectrum of polyphenylene using 1/8 the modulation ampli-
tude used to obtain spectrum of Fig. 11.
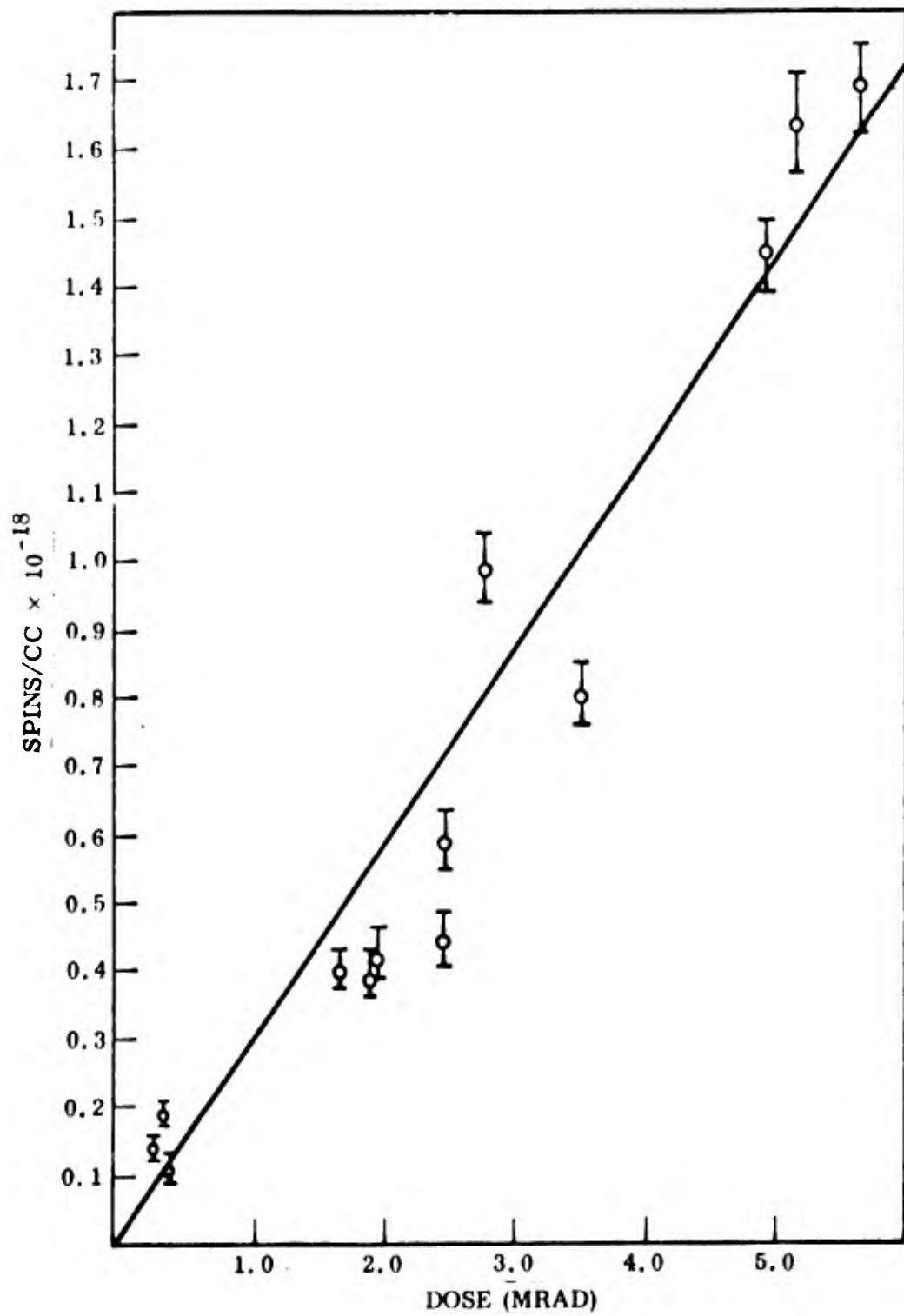
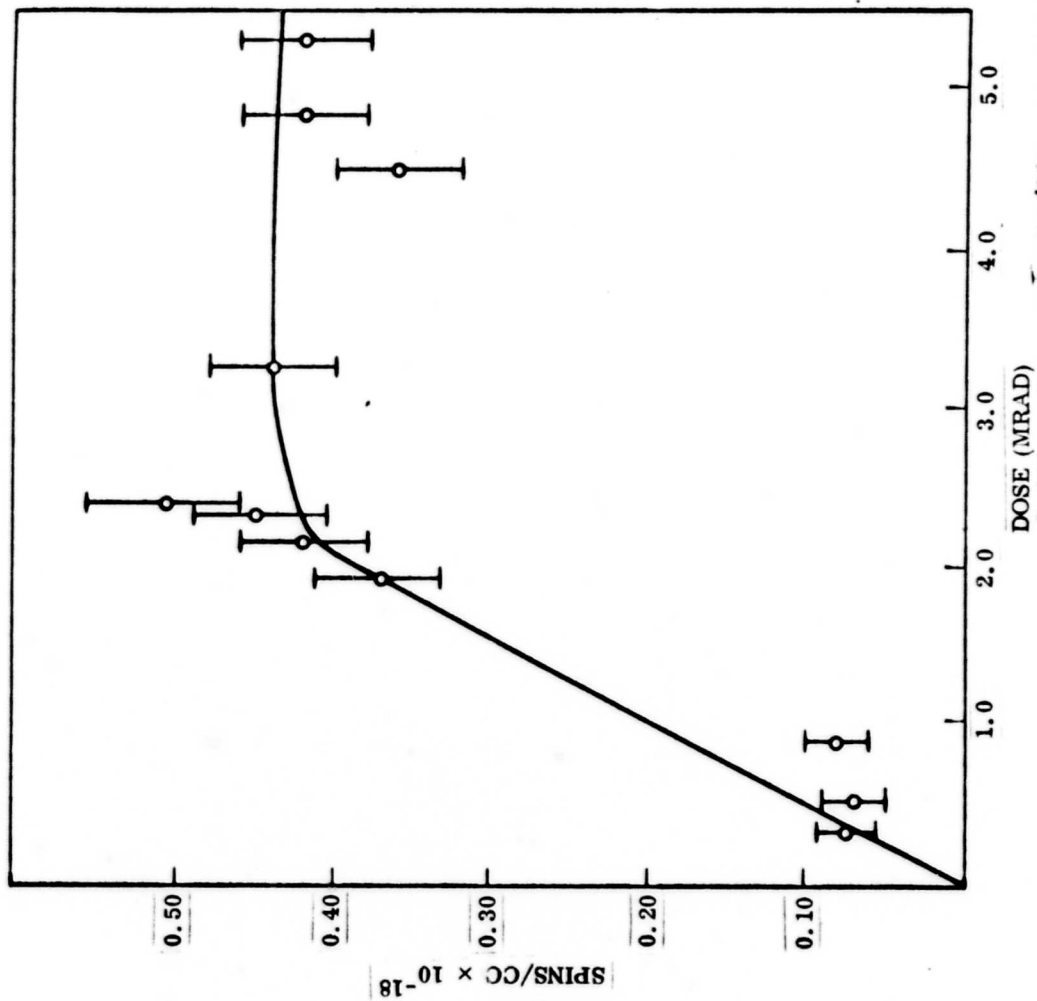Fig. 13  Free radical concentration versus dose for Teflon.

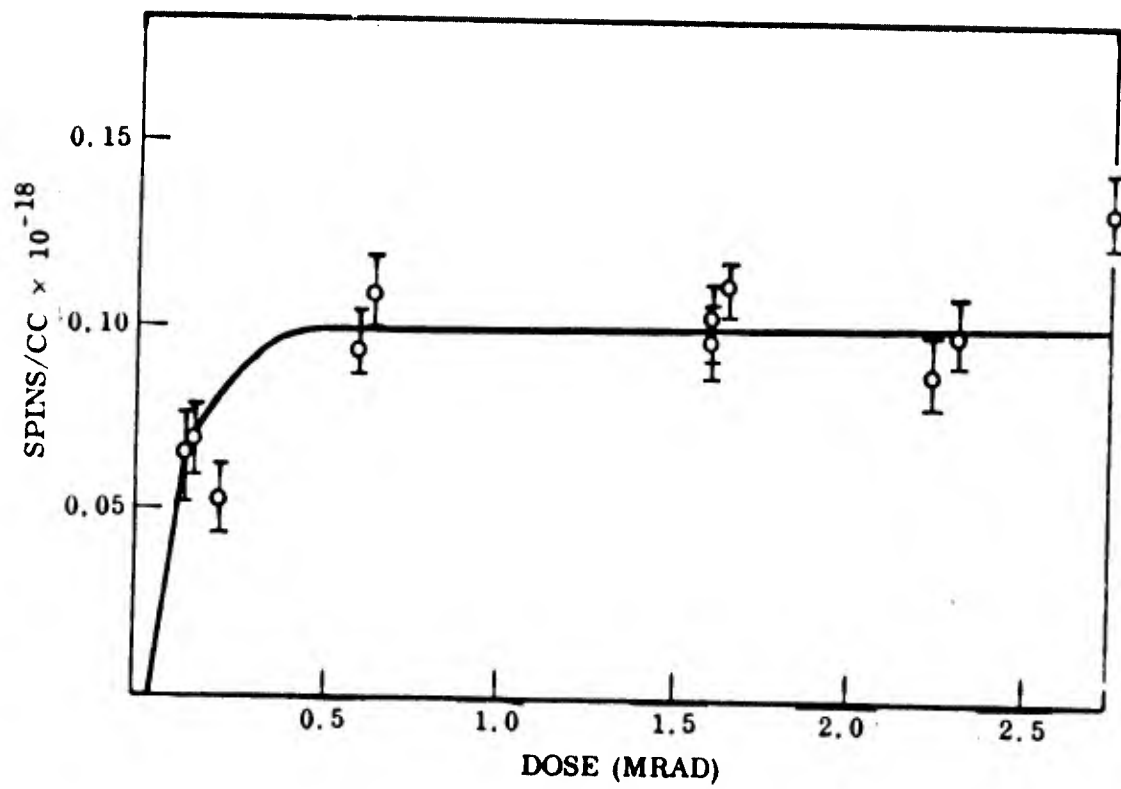Fig. 14 Free radical concentration vs dose for high density polyethylene.

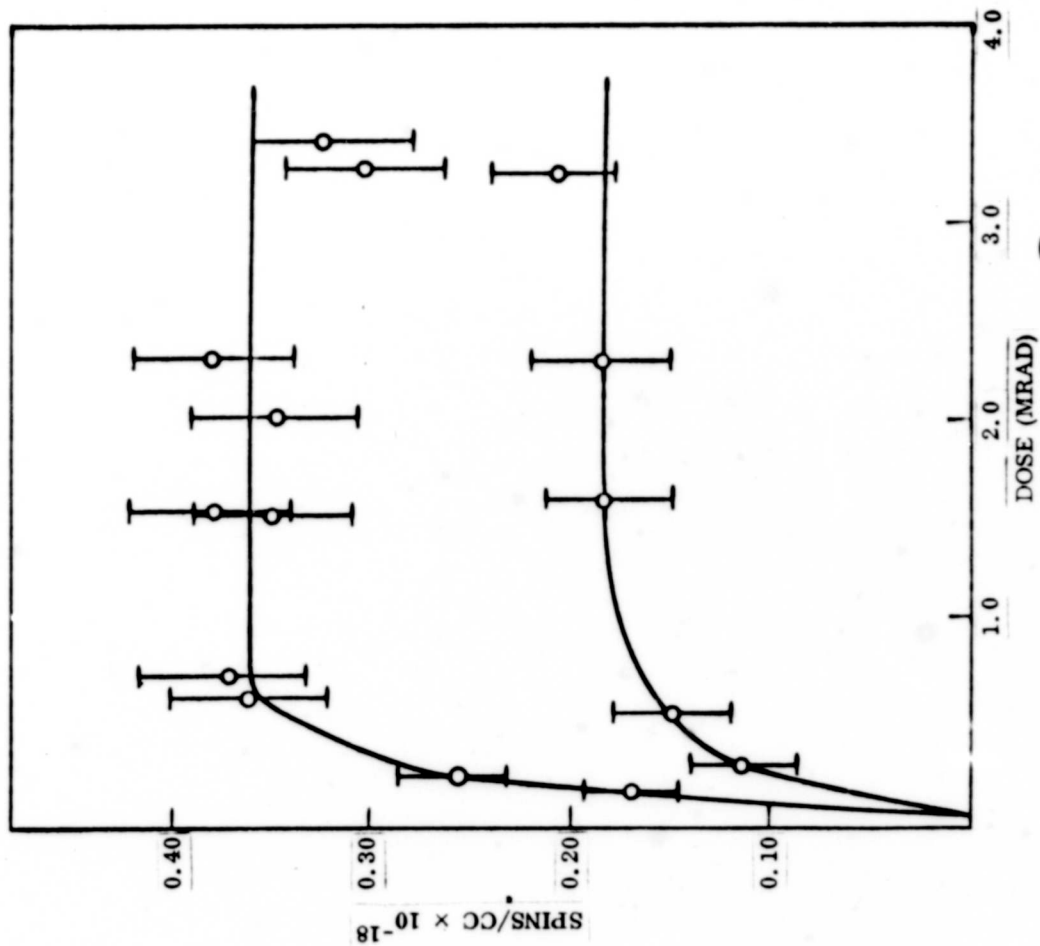Fig. 15. Free radical concentration vs dose for low density polyethylene.

Fig. 16 Free radical concentration versus dose for polyphenylene.